Electronic Supplementary Material (ESI) for Journal of Materials Chemistry A.

Supporting Information

Complementary Solvent Additives Tune the Orientation of Polymer Lamellae, Reduce the Sizes of Aggregated Fullerene Domains, and Enhance the Performance of Bulk Heterojunction Solar Cells

Chih-Ming Liu,[a] Yu-Wei Su,[a] Jian-Ming Jiang,[a] Hsiu-Cheng Chen,[a] Shu-Wei Lin,[a] Chun-Jen Su,[b] U-Ser Jeng*[b,c] and Kung-Hwa Wei*[a]

[a] Department of Materials Science and Engineering National Chiao Tung University 1001 Ta Hsueh Road, Hsinchu 30010, Taiwan, ROC

[b] National Synchrotron Radiation Research Center 101 Hsin-Ann Road, Science-Based Industrial Park Hsinchu 30077, Taiwan, ROC

[c] Department of Chemical Engineering, National Tsing Hua University, Hsinchu 30013, Taiwan, ROC

*Corresponding Author:

Prof. Kung-Hwa Wei

E-mail: khwei@mail.nctu.edu.tw

Prof. U-Ser Jeng

E-mail: usjeng@nsrrc.org.tw

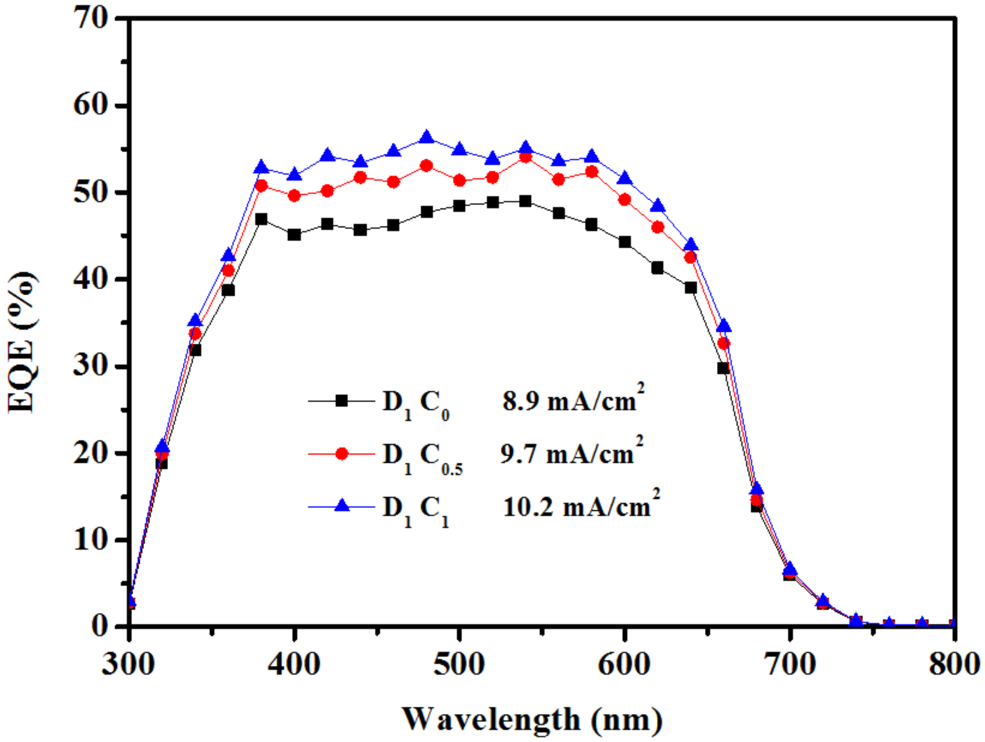

Figure S1. EQE curves of $PBTC_{12}TPD/PC_{71}BM$ blend films that had been processed in CF with the incorporation of additives from D_1C_0 to D_1C_1.

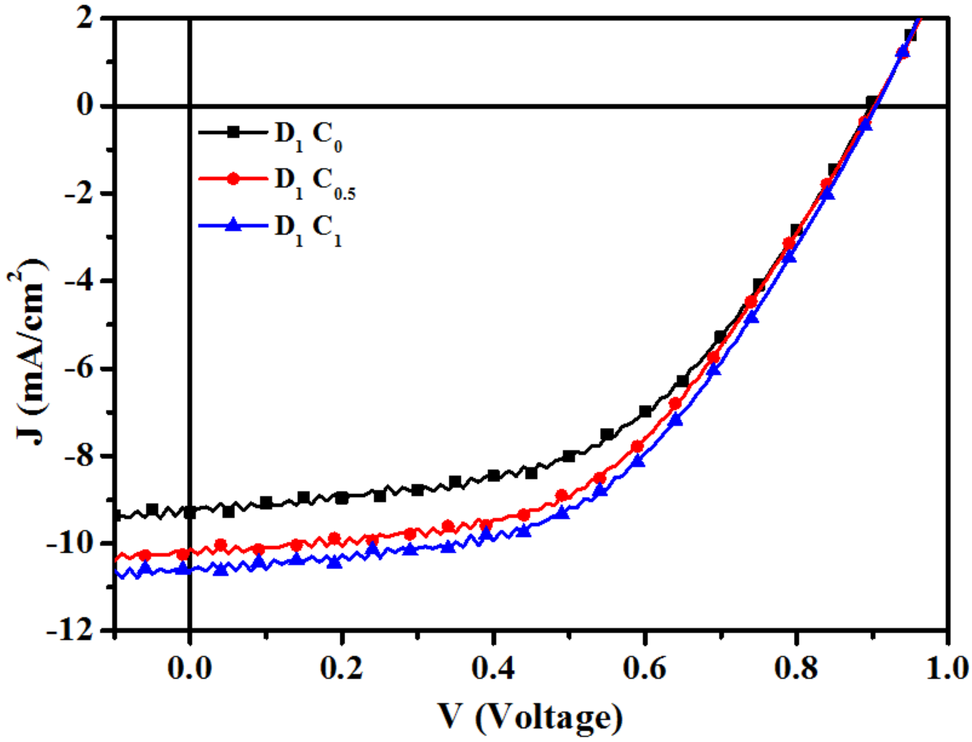

Figure S2. Current density–voltage curves of devices incorporating PBTC$_{12}$TPD/PC$_{71}$BM (1:1.5, w/w) active layers processed in CF with the incorporation of additives from D$_1$C$_0$ to D$_1$C$_1$.

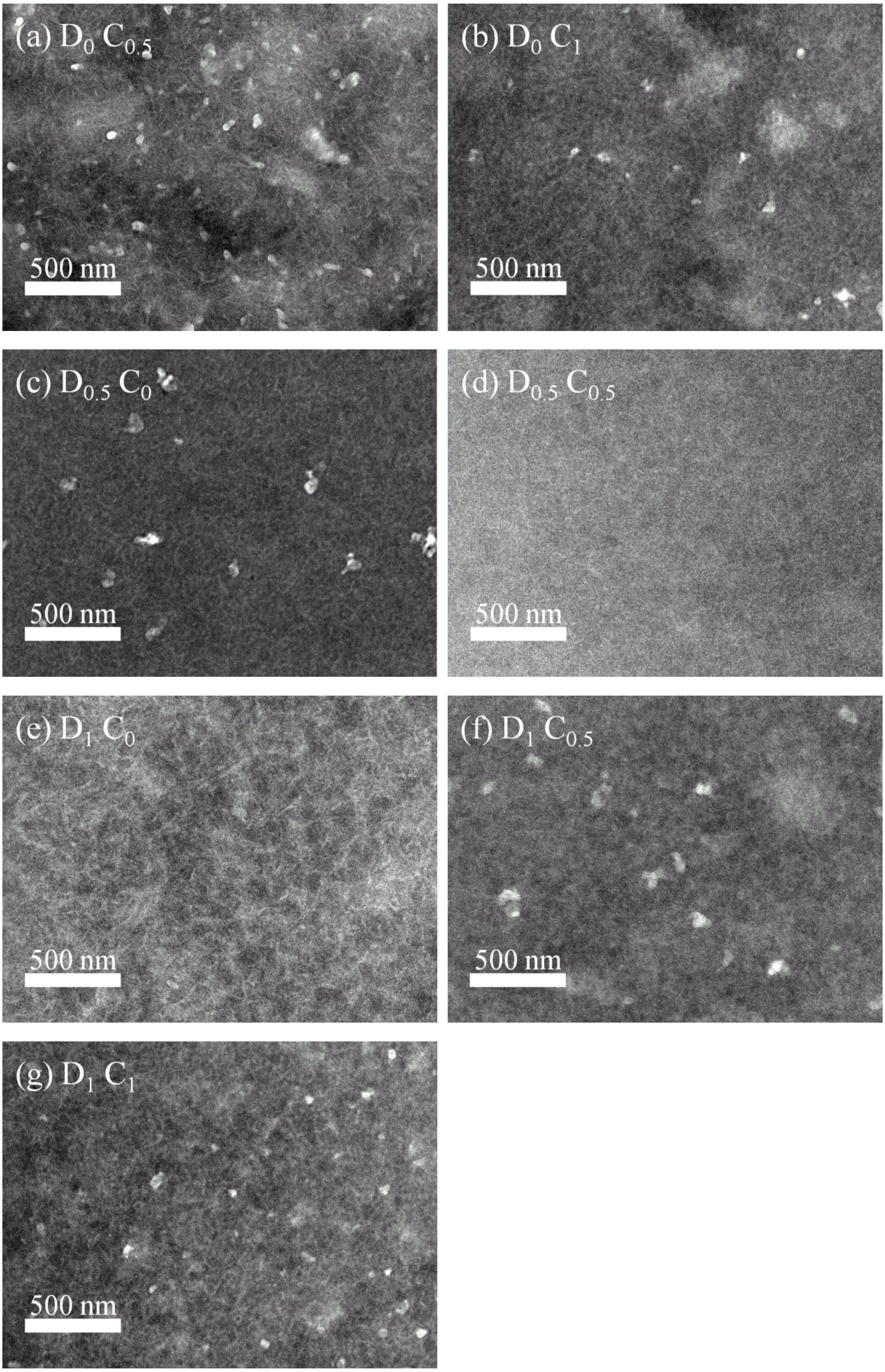

Figure S3. TEM images of $PBTC_{12}TPD/PC_{71}BM$ (1:1.5, w/w) films prepared (a) $D_0C_{0.5}$, (b) D_0C_1, (c) $D_{0.5}C_0$, (d) $D_{0.5}C_{0.5}$, (e) D_1C_0, (f) $D_1C_{0.5}$ and (g) D_1C_1 in the processing solvent.

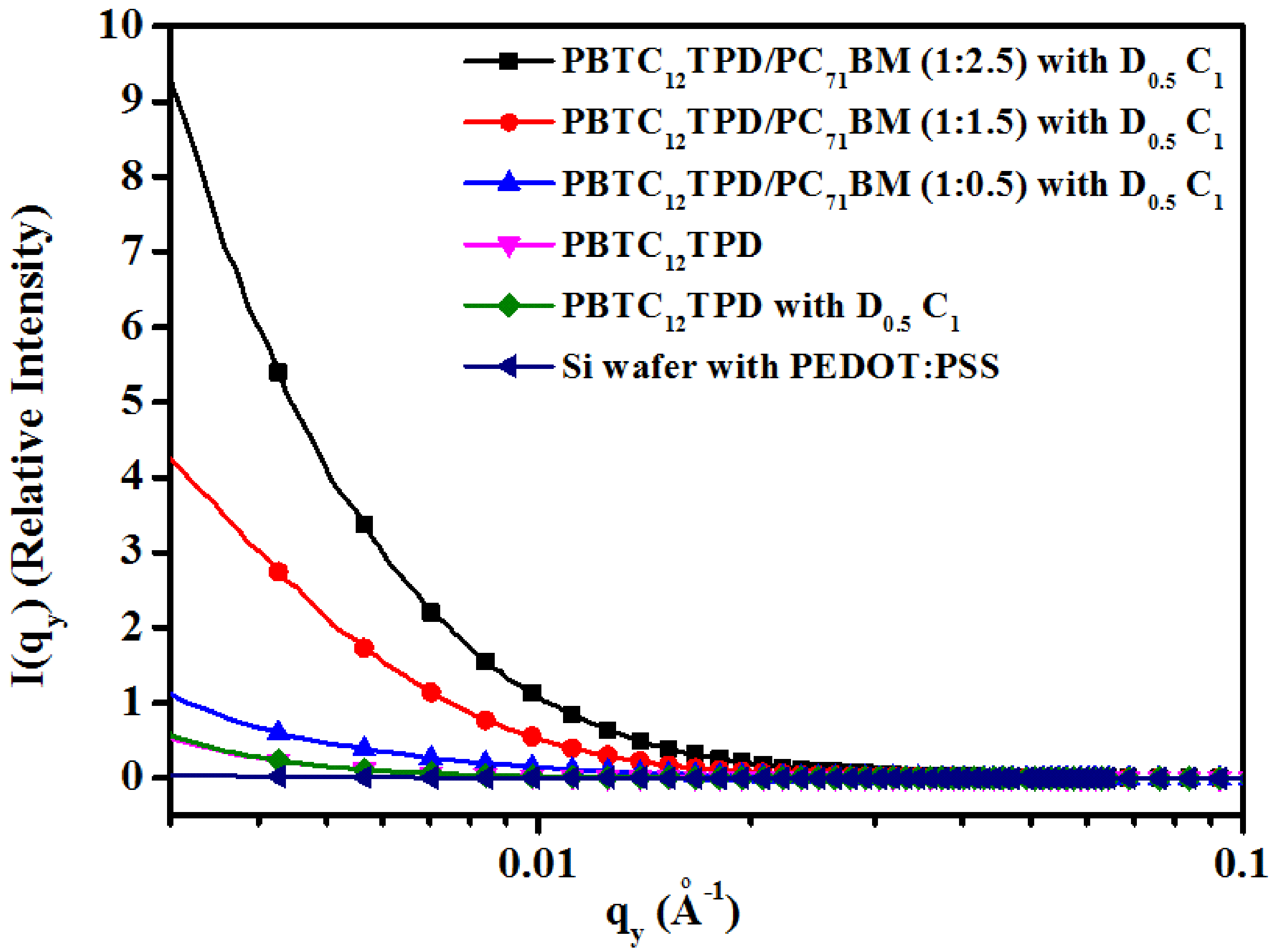

Figure S4. In-plane GISAXS profiles of spin-cast $PBTC_{12}TPD/PC_{71}BM$ films with various ratio 1:0.5, 1:1.5, 1:2.5 and pristine $PBTC_{12}TPD$ prepared in the absence of additives and in the presence of 0.5 vol% DIO and 1 vol% CN in the processing solvent.

We have performed additional GISAXS measurements of the blend films with the weight ratio of $PC_{71}BM$ varying from 0, 33, 60 to 70 wt%. Figure S4 shows that the intensity of the GISAXS profiles for the blend films increased with the weight ratio of $PC_{71}BM$ in the films, suggesting strongly that the weak slope breaks in the GISAXS profiles depend largely on $PC_{71}BM$ aggregation.

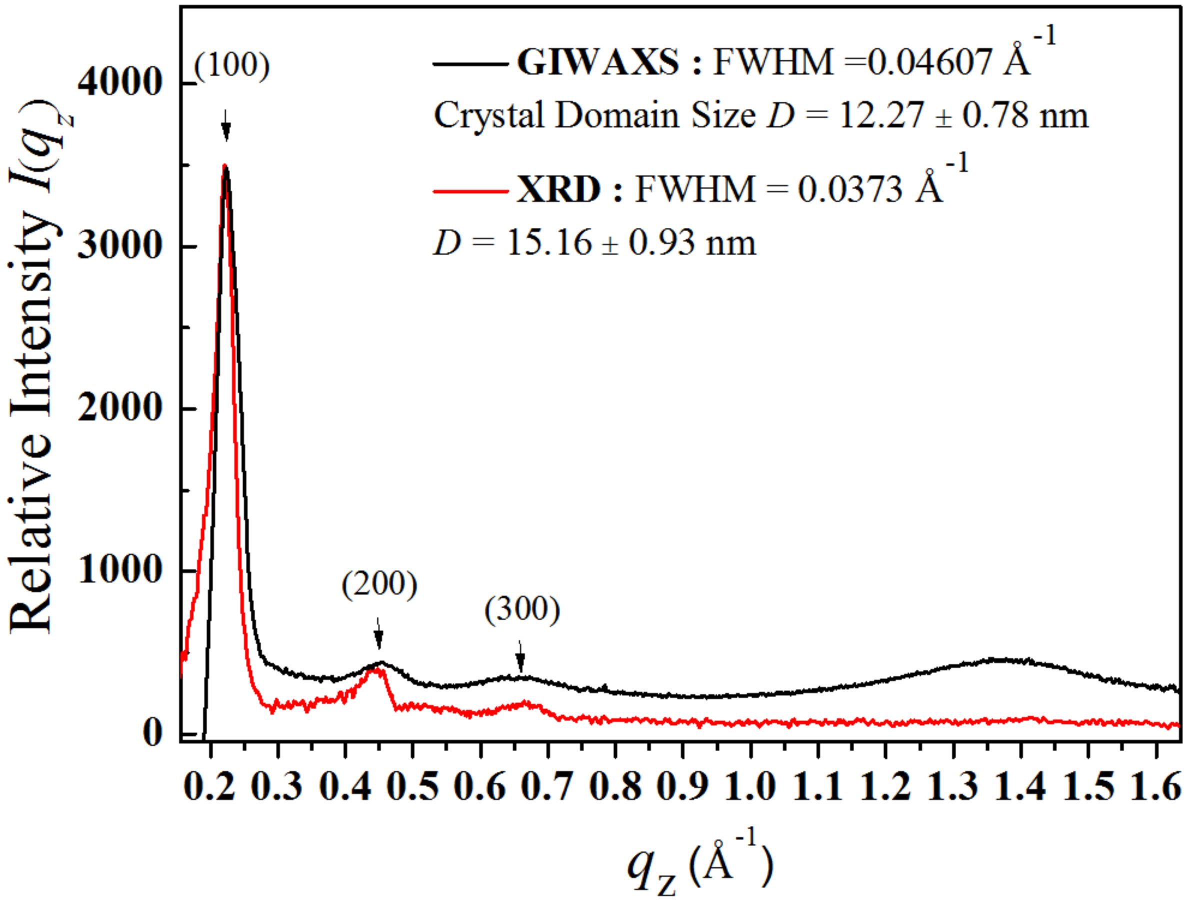

Figure S5. XRD profile along the azimuthal scan and the out-of-plane GIWAXS profile of spin-casted $PBTC_{12}TPD/PC_{71}BM$ (w:w/1:1.5) film without any additive. The full-width-half-maximum (FWHM) of the (100) peak of XRD or GIWAXS at 0.22 Å^{-1} and the corresponding crystal domain size are indicated.

The XRD profile overlapped approximately with the GIWAXS profile, especially in the low-*q* region for the (100) peak. Nevertheless, (100) peak width from the GIWAXS profiles is about 25% larger than that from XRD. We therefore, correct this systemic differences from the crystal domain size extracted from the GIWAXS (100) peak width, using the Sheerer equation. The results are summarized in Table 3. We note that the correction is systemic, and would not alter the relative trend of crystallization observed for the films processed under different conditions.

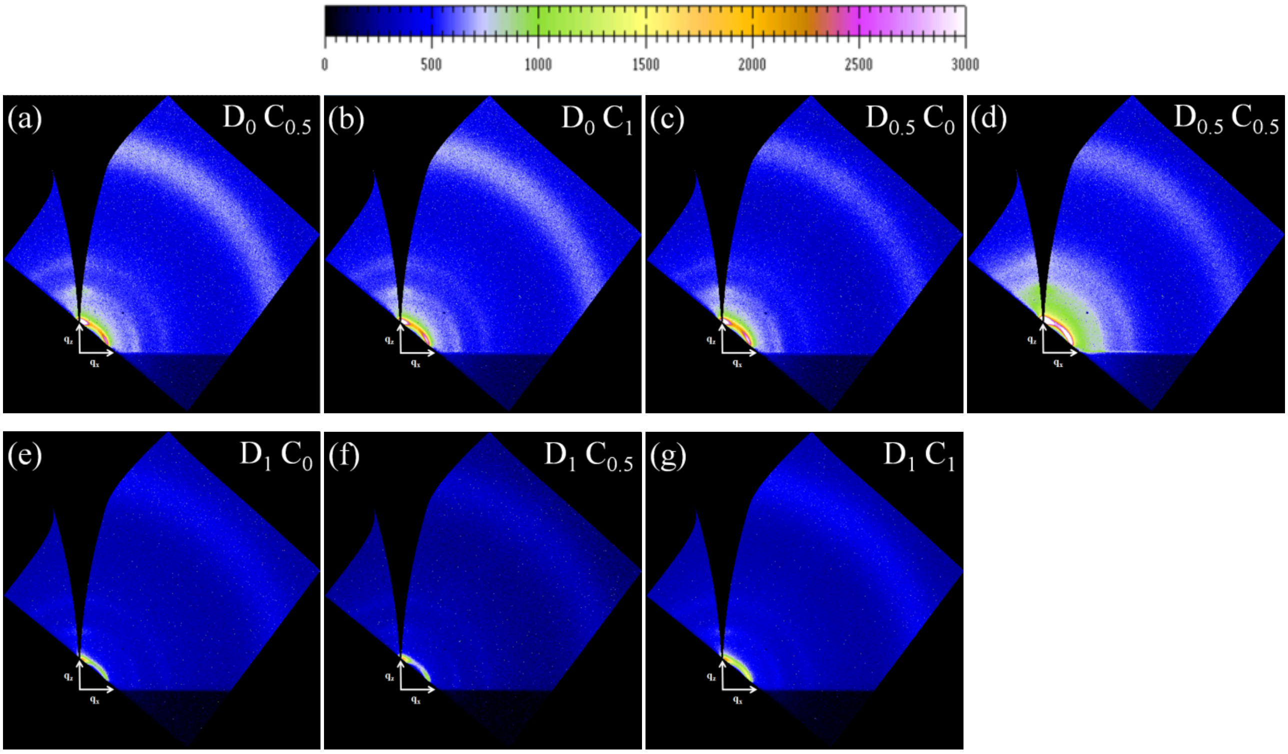

Figure S6. Pole figures of the 2D GIWAXS patterns of $PBTC_{12}TPD/PC_{71}BM$ (w:w/1:1.5) films of (a) $D_0C_{0.5}$, (b) D_0C_1, (c) $D_{0.5}C_0$, (d) $D_{0.5}C_{0.5}$, (e) D_1C_0, (f) $D_1C_{0.5}$ and (g) D_1C_1.

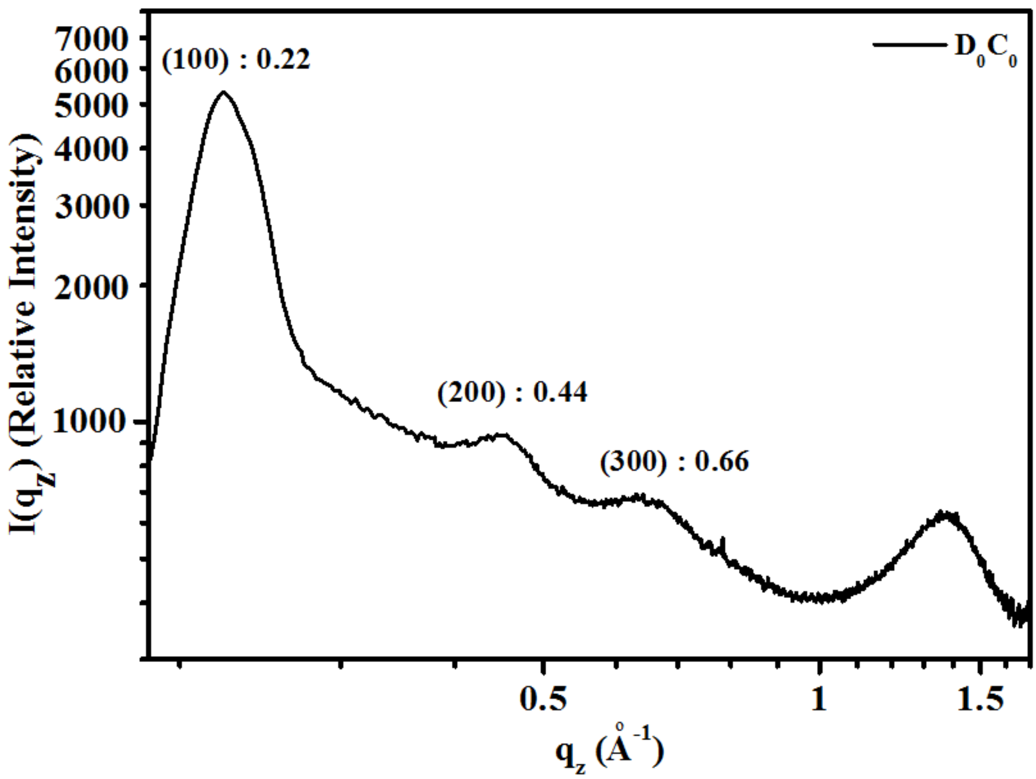

Figure S7. Background-subtracted GIWAXS profile of the PBTC$_{12}$TPD/PC$_{71}$BM film without any additives, exhibiting the first three lamellar peaks at 0.22 , 0.44, and 0.66 Å^{-1} as indicated.

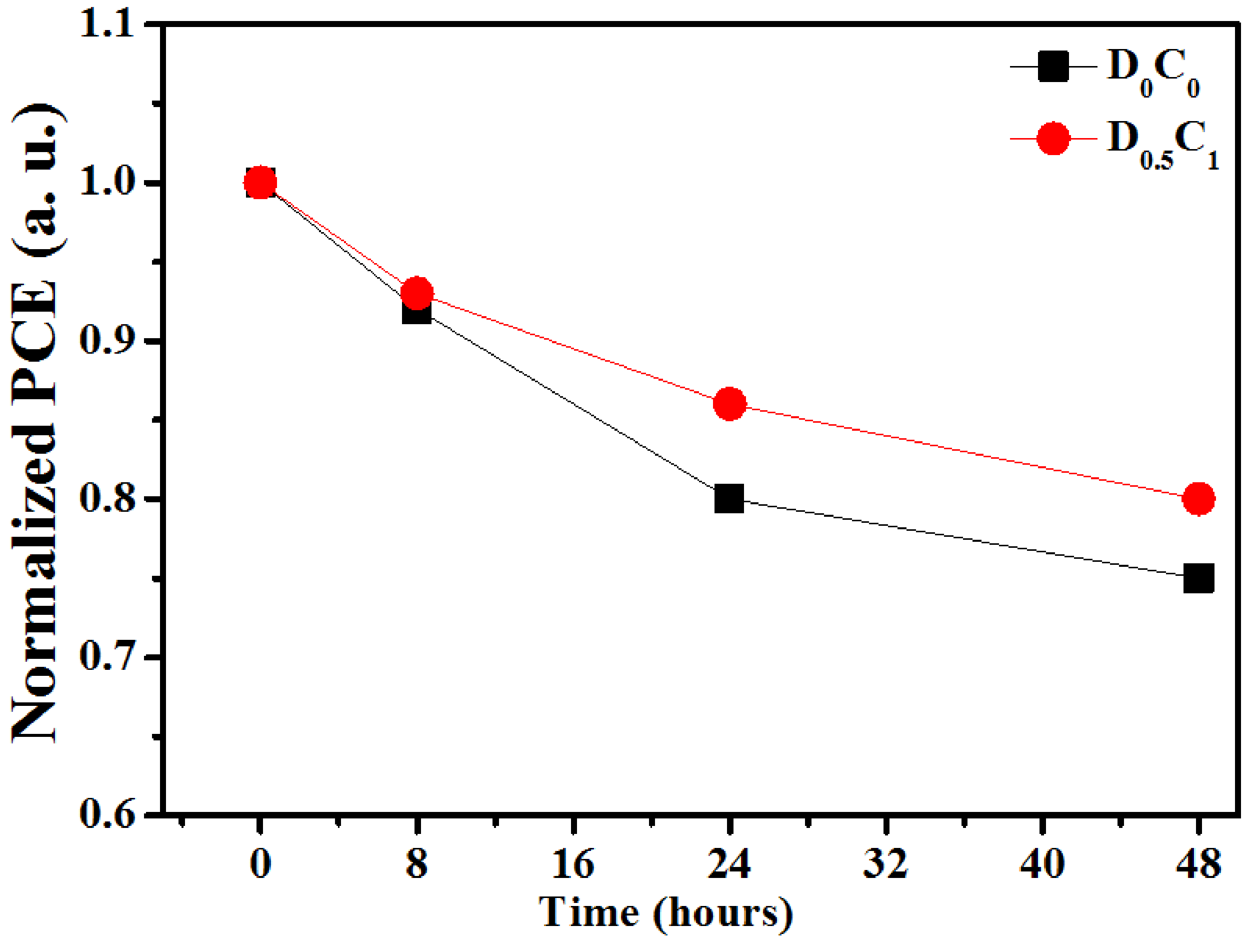

Figure S8. Stability of power conversion efficiency of $PBTC_{12}TPD/PC_{71}BM$ devices, respectively prepared without and with 0.5 vol% DIO and 1 vol% CN in the processing solvent.

We have carried out addition measurements on the stability of the devices. The results indicate that the device processed with the mixed additives could also have improved their PCE stability.

Table S1. Structural parameters the $PBTC_{12}TPD/PC_{71}BM$ films obtained by the model fitting.

Device	Additive Concentration (vol%)		PCBM Average Aggregate size $2R_a$ (nm)	PCBM Aggregate Size Polydispersity	Fractal Dimension D	Correlation Length (nm) ξ
	DIO	CN				
D_0C_0	0	0	6.0 ± 0.55	0.33	2.90 ± 0.019	67
$D_0C_{0.5}$	0	0.5	8.0 ± 0.62	0.30	2.67 ± 0.027	41
D_0C_1	0	1	8.1 ± 0.58	0.30	2.53 ± 0.025	51
$D_{0.5}C_0$	0.5	0	7.6 ± 0.47	0.30	2.53 ± 0.028	39
$D_{0.5}C_{0.5}$	0.5	0.5	11.0 ± 0.53	0.21	2.50 ± 0.036	38
$D_{0.5}C_1$	0.5	1	11.2 ± 0.56	0.25	2.35 ± 0.029	68
D_1C_0	1	0	13.2 ± 0.57	0.32	2.96 ± 0.014	490
$D_1C_{0.5}$	1	0.5	13.5 ± 0.63	0.30	2.93 ± 0.023	871
D_1C_1	1	1	14.0 ± 0.61	0.22	2.74 ± 0.038	1641

Since the present GISAXS profiles were measured in relative intensity scales, we have combined all the intensity related factors, such as the scattering contrast and volume fraction, into a single scaling parameter in Table S1. Note that the correlation lengths larger than 3000 Å were insensitively determined as lower-bound values, due to the limited low-q data available.